



Carbonation of slag concrete: Effect of the cement replacement level and curing on the carbonation coefficient – Effect of carbonation on the pore structure

Elke Gruyaert, Philip Van den Heede, Nele De Belie *

Magnel Laboratory for Concrete Research, Ghent University, Department of Structural Engineering, Technologiepark Zwijnaarde 904, B-9052 Ghent, Belgium

ARTICLE INFO

Article history:

Received 26 August 2011

Received in revised form 27 August 2012

Accepted 27 August 2012

Available online 12 September 2012

Keywords:

Blast-furnace slag

Carbonation

Microstructure

Curing

ABSTRACT

Concrete containing supplementary cementitious materials as, e.g. fly-ash (FA) or blast-furnace slag (BFS) is more vulnerable to carbonation than ordinary Portland cement concrete. In order to know whether carbonation-initiated corrosion is a risk within the life span of the concrete structure, the carbonation depth after several years (e.g. 50 years) is mostly predicted based on accelerated carbonation tests on young concrete specimens. However, these predictions do not take into account the positive effect of the continuing hydration of slag and fly-ash particles over a longer time.

In this study, accelerated carbonation tests (10 vol.% of CO₂) were performed on concrete specimens containing different amounts of blast-furnace slag (slag-to-binder ratios of 50%, 70% and 85%) after different curing times (1, 3, 6 or 18 months). Based on these tests, a new method, which takes into account the effect of the ongoing hydration, is described in order to predict the carbonation depth of these special types of concrete over a long time more realistically. The tests revealed that, although BFS concrete has a lower carbonation resistance than OPC concrete, the depth of carbonation at the end of the concrete's life (50 years) can still be acceptable in normal environments.

© 2012 Elsevier Ltd. All rights reserved.

1. Introduction

The use of supplementary cementitious materials is one of the current practices, to make the cement and concrete industry more environmentally-friendly. However, ordinary Portland cement (OPC) is a hydraulic product while blast-furnace slag (BFS) and fly-ash (FA) are respectively latent-hydraulic and pozzolanic by-products. Partial replacement of OPC by BFS or FA alters thus the reaction kinetics and reaction degrees. Former research already showed that the microstructure of BFS and FA concrete develops slower (the hydration is slower, initial and final setting times are prolonged, the strength develops slower, the hydration degree of BFS/FA is low for mixes with high replacement levels, etc.) and the durability behaviour is different from that of OPC concrete [1–6].

In spite of this time-dependent effect, accelerated degradation tests are mostly executed at an age of 28 days on a lab scale (as is done for OPC concrete), in order to evaluate the performance of BFS/FA concrete. This means that the beneficial effect of ongoing hydration of the alternative binders over a longer time period is not taken into account. When these values are used for service life predictions, the concrete's performance will be underestimated. In a more recent Belgian standard (NBN B15-100 (2008)) which deals with the equivalent performance concept for attestation of the

suitability of alternative binder systems, the former issue is already considered since a curing time of 55 days is generally prescribed in this standard.

While accelerated tests at young ages can give unrealistic results, some concrete structures are already exposed to aggressive substances almost immediately after casting. In those cases, testing at later ages can give too favourable and also unrealistic test results.

In this paper, a method to determine a time-dependent carbonation coefficient is proposed. Moreover, the carbonation resistance of BFS concrete is discussed and the influence of replacement level and curing time are considered. Finally, the effect of carbonation on the pore structure of OPC and BFS concrete is discussed.

2. Materials and methods

2.1. Materials

2.1.1. Concrete mix design

Concrete mixes containing different amounts of BFS were produced. The slag-to-binder ratio (s/b) amounted to 0% (S0), 50% (S50), 70% (S70) or 85% (S85), the water-to-binder ratio (w/b) was 0.5. The composition for 1 m³ concrete is tabulated in Table 1. CEM I 52.5 N, complying with the European Standard EN 197-1 (2000), was used and the slag was added to the concrete mix as a separate component. The characteristics of the cement and slag are summarized in Table 2.

* Corresponding author. Tel.: +32 9 264 55 22; fax: +32 9 264 58 45.

E-mail address: Nele.Debelie@UGent.be (N. De Belie).

Table 1Concrete composition of S0, S50, S70 and S85 (kg/m³ concrete).

	S0	S50	S70	S85
OPC	350	174	105	52
BFS	0	174	244	295
Water	175	174	174	174
Sand 0/4	791	788	787	785
Gravel 2/8	425	423	423	422
Gravel 8/16	618	616	615	614

Table 2Chemical composition (%) and Blaine fineness (m²/kg) of the Portland cement and blast-furnace slag.

	OPC	BFS
CaO	63.12	42.64
SiO ₂	18.73	33.86
Al ₂ O ₃	4.94	8.91
Fe ₂ O ₃	3.99	0.69
MgO	1.02	7.39
K ₂ O	/	0.52
Na ₂ O	/	0.28
SO ₃	3.07	1.62
S ²⁻	/	0.72
CO ₂	0.65	0.36
Mn	/	0.19
Cl ⁻	/	0.01
Insoluble residue	0.21	0.16
LOI	2.12	/
Blaine fineness	359	397

/ Value not determined.

2.1.2. Curing

The cubes with a side length of 100 or 150 mm were demoulded after 1 day and cured in a climate room at a temperature of (20 ± 2) °C and a relative humidity (RH) higher than 95% for 1, 3, 6 or 18 months. Since diffusion of CO₂ is strongly slowed down for climates with a RH higher than 70% [7], the hydration of cement and slag can proceed unhindered. This way, the influence of ongoing hydration on the carbonation resistance can be investigated.

2.2. Accelerated carbonation test

2.2.1. Measurement

Before the start of the accelerated carbonation test (after 1, 3, 6 or 18 months curing), the initial value of the carbonation depth (x_0) was determined by the dyeing method as explained below. Subsequently, all sides of the concrete cubes (100 × 100 × 100 mm), except the one (moulding surface) which will be exposed to the environment with high CO₂ concentration, were coated (Fig. 1A). That way, one-dimensional penetration of CO₂ from one side of the cube was assured. Three concrete specimens of each mix were then exposed to an atmosphere containing 10 vol.% CO₂ at 20 °C and 60% RH (Fig. 1B). After 2, 4, 8, 16 and 24 weeks, the carbonation depth was determined by spraying phenolphthalein solution on a fresh saw cut (Fig. 1C and F). Since the colour of the indicator turns purple at a pH above 9.2 [8], non-carbonated zones are coloured while carbonated zones are colourless (Fig. 1G). The carbonation depth was measured at nine different places (10 mm distance between the measurements) to the nearest millimetre (Fig. 1G). The other saw-cut was coated again (Fig. 1D and E) and

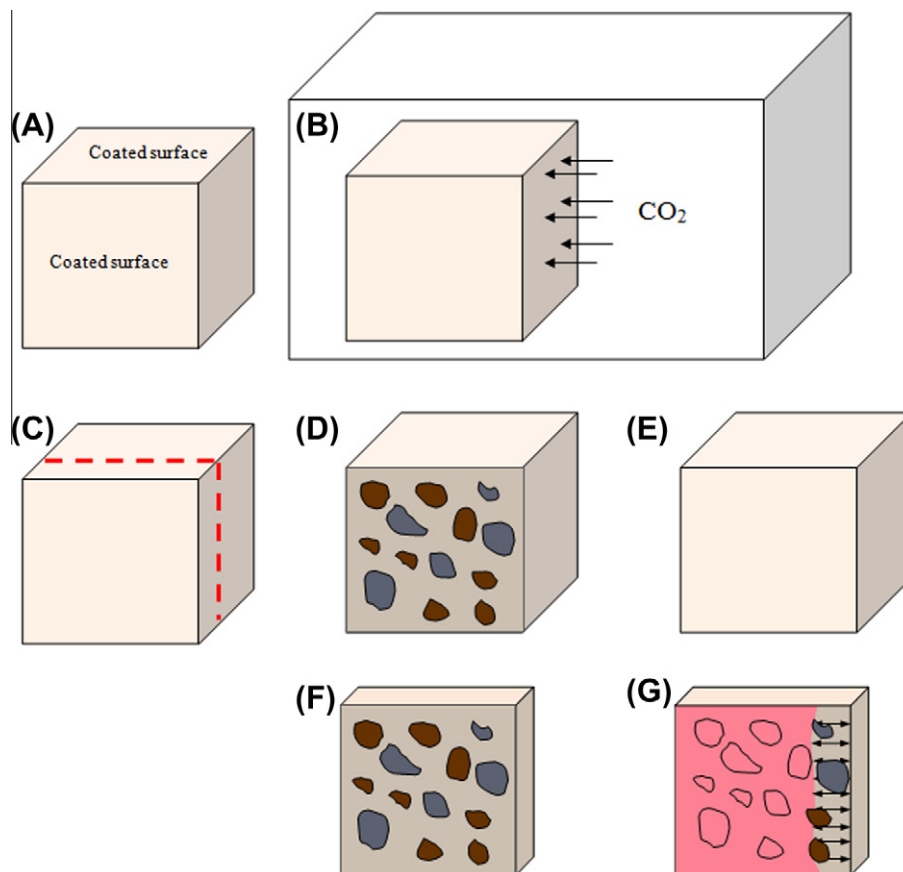


Fig. 1. Accelerated carbonation test – (A) all surfaces, except the one which will be exposed to the CO₂ environment, are coated; (B) specimens are placed in a carbonation chamber with 10 vol.% CO₂, 20 °C and 60% RH – CO₂ can migrate in concrete via the non-coated surface; (C) a slice of 1 cm is sawn; the sawn surface (D) will be coated again (E); phenolphthalein solution will be sprayed on the fresh sawn surface (F); carbonated zones are colourless (G) and non-carbonated zones colour purple (G) after spraying phenolphthalein solution.

the specimen was placed in the carbonation chamber until the next measurement.

Additionally, thin sections were made from a limited number of test specimens (cured for 18 months) and the carbonation depths obtained by both methods ((i) spraying of phenolphthalein solution on a freshly cut surface and (ii) optical microscopy) were compared.

Furthermore, some researchers claim that for the determination of the carbonation depth by the dyeing method broken surfaces have to be used, and saw-cuts are not always suitable [9]. Therefore, a comparison is made between the carbonation coefficients calculated from tests on sawn and broken surfaces (results derived from the tests described in Sections 2.3 and 3.2).

2.2.2. Processing

To calculate the carbonation coefficient A (mm/ $\sqrt{\text{day}}$), the penetration depth x (mm) was written as a function of the square root of the exposure time t (days) (Eq. (1)) [10].

$$x = x_0 + A \cdot \sqrt{t} \quad (1)$$

The carbonation coefficients are based on accelerated carbonation tests, which expose the specimens to a 10 vol.% CO_2 environment. In real circumstances, the CO_2 content of air ranges between 0.03% and 0.3% and can exceptionally increase up to 1% [7]. To take into account this concentration (c) difference

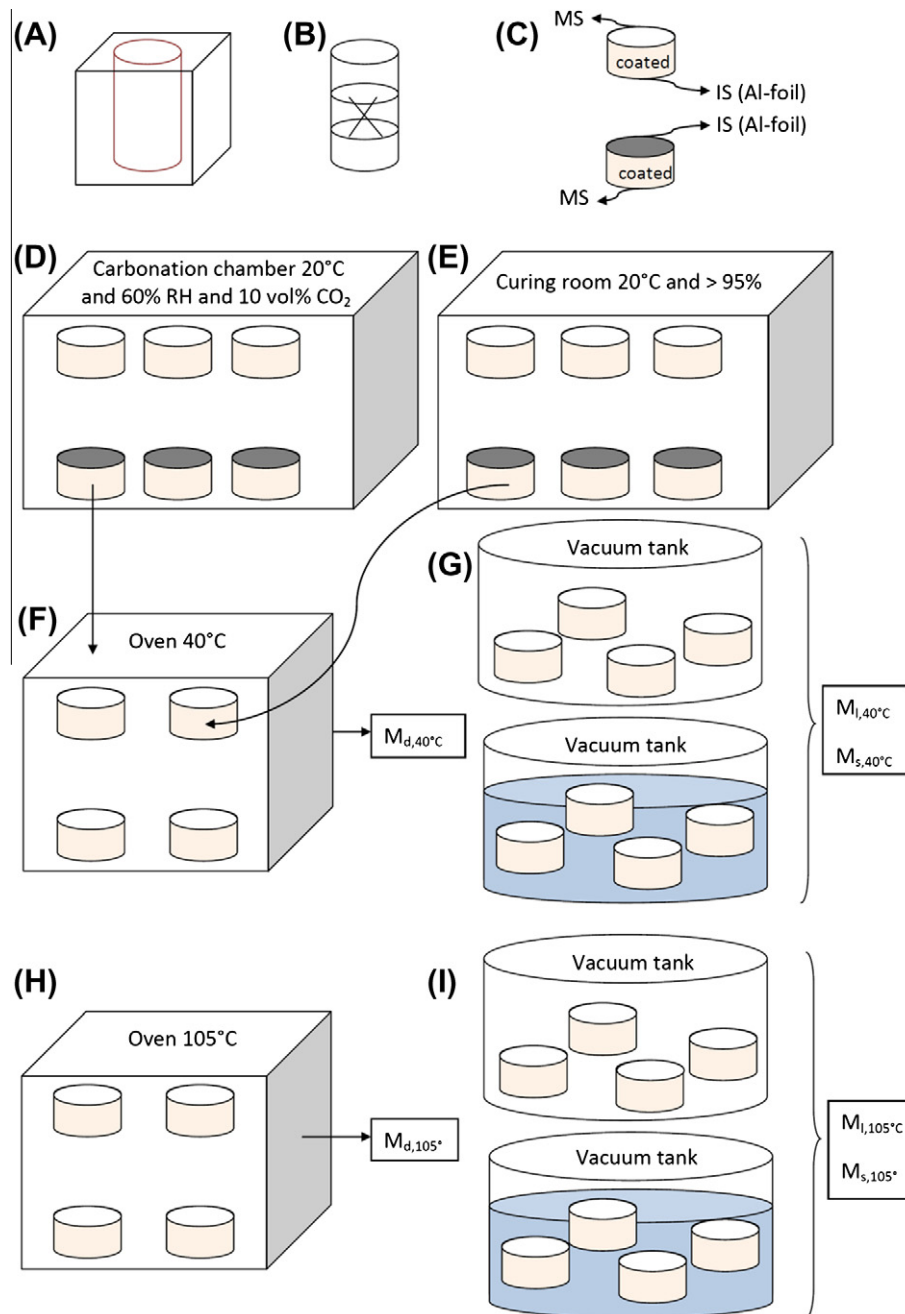


Fig. 2. Vacuum saturation test – (A) cores are drilled from the cubes; (B) the core is sawn into three identical cylindrical specimens; (C) the circumferential surfaces are coated and one top surface (=IS) is covered with aluminium foil (MS = moulding surface; IS = interior surface); part of the specimens are placed in a carbonation chamber with 10 vol.% CO_2 , 20 °C and 60% RH (D), another part in a climate chamber at 20 °C and >95% RH (E); (F) after 4, 16 and 24 weeks, specimens are dried in an oven at 40 °C; (G) vacuum saturation; (H) specimens are dried in an oven at 105 °C; (I) vacuum saturation.

between the accelerated tests (subscript *a*) and the real environment (subscript *r*), the values of *A* were converted according to formula (2) [11].

$$\frac{A_a}{A_r} = \frac{(x - x_0)_a}{(x - x_0)_r} = \sqrt{\frac{c_a}{c_r}} \quad (2)$$

2.3. Influence of carbonation on the pore structure

2.3.1. Measurement

At the time of testing (1, 3, 6 and 18 months), cylindrical test specimens (*h* 50 mm; \varnothing 100 mm) were drilled (Fig. 2A) and sawn (Fig. 2B) from the cubes (150 × 150 × 150 mm). Only the cylinders containing a moulding surface were considered. Subsequently, the circumferential surfaces were coated (Fig. 2C) and the interior surfaces were covered with an aluminium foil, so that CO₂ can only penetrate the concrete from the moulding surfaces (Fig. 2C).

Per mix, 3 × 2 concrete cylinders were exposed to a high CO₂ concentration (10 vol.%) at a temperature of 20 °C and 60% RH (Fig. 2D), while another 3 × 2 test specimens were further stored in the climate room at (20 ± 2) °C and a RH higher than 95% (Fig. 2E). After 4, 16 and 24 weeks, 1 × 2 specimens were removed from each of the climate chambers and the aluminium foil was removed. The specimens were first dried at 40 °C for 14 days (dry mass = *m_d*) (Fig. 2F) and were then subjected to a vacuum saturation test according to the standard NBN B05-201 (paragraph 6.1-1976) (Fig. 2G). The specimens were placed in a vacuum with a residual pressure of 2.7 kPa for 2.5 h. Thereafter, water was added at a rate of 5 cm/h until the specimens were completely immersed. The air pressure was re-established and the cylinders were stored under water for 24 h. Finally, the mass of the specimens under water (*m_i*) and the saturated mass (*m_s*) were determined. Subsequently, the specimens were subjected to a second vacuum saturation test (Fig. 2I), preceded by drying at 105 °C (Fig. 2H).

After the vacuum saturation tests, the test specimens were split and the carbonation depth of each of the specimens was determined by spraying a phenolphthalein solution on the freshly broken surface.

In addition, the open porosity of uncarbonated reference specimens (*h* 50 mm; \varnothing 100 mm) was determined after a curing period of 1, 3, 6 or 16 months, according to the method described above.

2.3.2. Processing

The open porosity ($\varphi_{40^\circ\text{C}}$ and $\varphi_{105^\circ\text{C}}$) of carbonated and non-carbonated test specimens was calculated (Eq. (3)). The obtained results were related to the depth of the carbonation front and the cement replacement percentage in the mix.

$$\varphi_{40^\circ\text{C}} = \frac{m_{s,40^\circ\text{C}} - m_{d,40^\circ\text{C}}}{m_{s,40^\circ\text{C}} - m_{l,40^\circ\text{C}}} \quad (3)$$

$$\varphi_{105^\circ\text{C}} = \frac{m_{s,105^\circ\text{C}} - m_{d,105^\circ\text{C}}}{m_{s,105^\circ\text{C}} - m_{l,105^\circ\text{C}}}$$

3. Results and discussion

3.1. Influence of the cement replacement level and curing on the carbonation resistance

In Fig. 3, the evolution of the carbonation depth as a function of time is presented for concrete specimens containing different amounts of BFS (*s/b* = 0, 0.5, 0.7 and 0.85), cured for 1, 3, 6 or 18 months at 20 °C and a RH > 95% and subsequently exposed to a 10 vol.% CO₂ environment. The carbonation front was determined after spraying phenolphthalein solution on a freshly sawn surface. In Fig. 4, the carbonation coefficients *A*, estimated by formula (1), are presented as a function of the curing age for the different concrete mixes. The values of *x*₀ are considered to be 0, except for S70 – 1 M and S85 – 1 M since these mixes showed a carbonation depth of ~1.5 mm before the start of the accelerated carbonation test.

3.1.1. Cement replacement level

As can be seen in both figures, the reference concrete (which is consistent with the prescriptions of EN 206-1 (2000) for an XC environment) shows no carbonation and the carbonation coefficient is (almost) zero. However, the carbonation depths and consequently the carbonation coefficients increase with increasing BFS content. This is not surprising: the pH of BFS pore solutions is already low and since CO₂ preferentially reacts with CH (which is only present in small amounts), the pH is rapidly reduced below the colour change of the phenolphthalein indicator. Moreover, the gas permeability of the concrete mixes increases with increasing BFS content [12] and the carbonation reaction in BFS concrete mixes leads to a coarsening of the pore structure (see Section 3.2) allowing CO₂ to penetrate more easily in the concrete.

3.1.2. Curing time

For BFS concrete, the values of *A* decrease strongly when curing time increases from 1 to 3 months, while (almost) no change is recorded afterwards. This means that continuous curing over periods longer than 1 month can still significantly increase the durability properties of BFS concrete, but curing for periods longer than 3 months does not considerably affect the resistance to carbonation anymore.

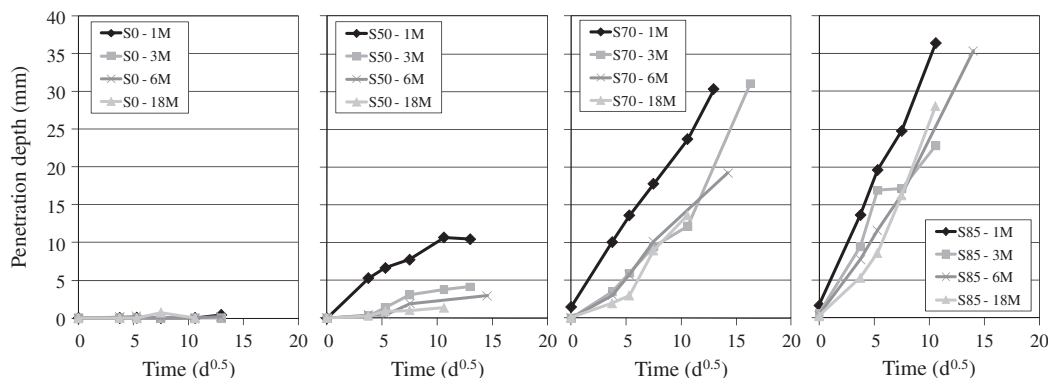


Fig. 3. Evolution of the carbonation depth as a function of exposure time for concrete mixtures (cured for 1, 3, 6 or 18 months at ~20 °C and >95% RH) containing different amounts of OPC and BFS, exposed to an environment containing 10 vol.% CO₂.

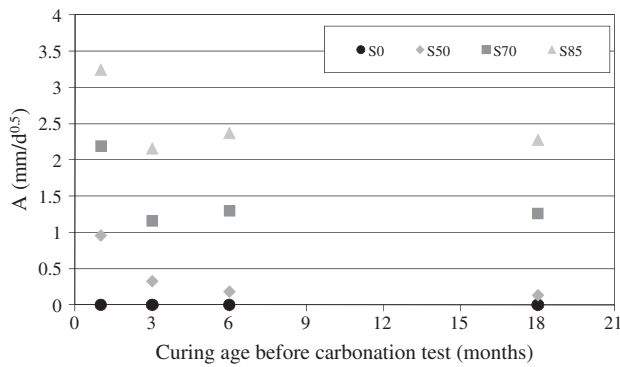


Fig. 4. Change of the carbonation coefficient A as a function of the curing period before exposure to a climate containing 10 vol.% CO_2 at 20 °C and 60% RH.

Table 3

Carbonation coefficient ($\text{mm}/\sqrt{\text{day}}$) calculated based on phenolphthalein spraying on broken or sawn surfaces.

Curing time	1 month	3 months	18 months
S0 – broken surface	0	0	0
S0 – sawn surface	0	0	0
S50 – broken surface	0.7	0.3	0.3
S50 – sawn surface	0.9	0.3	0.1
S70 – broken surface	1.4	0.9	1.2
S70 – sawn surface	2.2	1.2	1.3
S85 – broken surface	3.2	2.0	2.2
S85 – sawn surface	3.2	2.2	2.3

3.1.3. Sawn versus broken surfaces

In Table 3, a comparison is made between the carbonation coefficients, calculated after determination of the carbonation depth by phenolphthalein spraying on sawn and broken surfaces at different times. The values for sawn surfaces correspond to the carbonation coefficients of Fig. 4. The carbonation coefficients for broken surfaces are calculated based on the results mentioned in Section 3.2. The values in Table 3 clearly show that the influence of

the preparation method (sawing–splitting) on the obtained carbonation coefficients is rather limited or nil (except S70 after 1 month curing). Consequently, it can be concluded that saw-cuts are found suitable and the corresponding carbonation coefficients are reliable.

3.1.4. Measuring technique

A phenolphthalein indicator only indicates whether the pH is higher or lower than ~ 9 but beyond this colour change boundary, concrete can be partially carbonated. In these zones, the pH is also reduced, but remains higher than ~ 9 . Since other researchers ([13] cited by [14]) mentioned that steel corrosion was already observed at pH values higher than 9, the position of the carbonation front was examined more in detail by optical microscopy. Under crossed polars, this technique allows to distinguish the carbonated and non-carbonated zones by the colour. As can be seen in Fig. 5, carbonated zones stain lighter and although the front can be easily determined, the margins are irregular (e.g. isolated uncarbonated zones (Fig. 5 – S50), a deeper carbonation front around some aggregates (Fig. 5 – S70)).

Nevertheless, mean values for the carbonation depths as obtained by both techniques (phenolphthalein spraying (PS) and optical microscopy (OM)) are compared in Table 4. For the reference mixtures, which showed no carbonation based on PS, a very small (0.1–0.7 mm) carbonated zone could be detected by OM. However, no logical relation with the exposure time could be found. This is not so surprising since: (i) the carbonation front is positioned near the surface (very small depths), (ii) concrete is not a homogeneous material, (iii) thin sections are small ($35 \times 45 \text{ mm}$) and only a limited amount of measurements (4 or 5) could be taken over the width. For the BFS concrete mixtures, the carbonation front as obtained by OM is in general located deeper. Deviations up to 3 mm were registered. However, the same remarks as mentioned above had to be taken into consideration.

3.1.5. Prediction of the carbonation depth within the concrete's life span

In Table 5, the depths of the carbonation fronts after 1 and 50 years are estimated based on the above mentioned carbonation

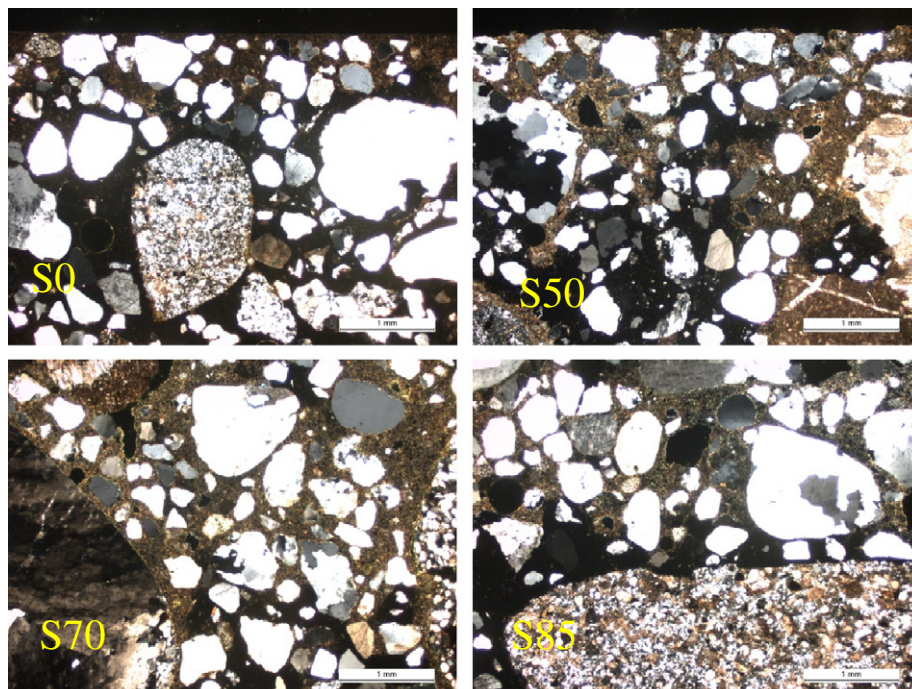


Fig. 5. Visualisation of the carbonation front (downward CO_2 ingress) by optical microscopy (S0, S50, S70 and S85 (18 M)). Carbonated zones coloured 'brown' (—=1 mm). (For interpretation of the references to colour in this figure legend, the reader is referred to the web version of this paper.)

Table 4

Comparison between the carbonation front (in mm) obtained by phenolphthalein solution (PS) and optical microscopy (OM) for specimens stored in a climate room at 20 °C and >95% RH (CR) or in a carbonation cabinet (CC) for 4, 8 or 16 weeks (test age = 18 months).

Exposure time		S0		S50		S70		S85	
		PS	OM	PS	OM	PS	OM	PS	OM
4 weeks	CR	0	0.5	0	0.1	1.2	1.4	1.6	2.0
	CC	0	0.7	0.8	0.5	2.8	2.0	8.6	10.8
8 weeks	CR	0	0.7	0	0.4	1.0	1.8	1.9	0.5
	CC	0	0.3	1.0	2.0	9.0	9.6	16.3	17.5
16 weeks	CR	0	0.1	0	0.6	2.2	5.4	2.8	2.5
	CC	0	0.2	1.4	3.2	13.2	12.2	28.1	24.2

Table 5

Estimate of the carbonation depth (in mm) (based on carbonation coefficients obtained after curing for 1 month (A1) or 3 months (A3)) after 1 and 50 years exposure to a 0.03% or 0.3% CO₂ environment.

	S0	S50	S70	S85
X ₁ year, A1, 0.03%	0	1.0	2.29	3.39
X ₅₀ year, A1, 0.03%	0	7.07	10.17	23.96
X ₁ year, A3, 0.03%	0	0.34	1.21	2.26
X ₅₀ year, A3, 0.03%	0	2.43	8.57	15.95
X ₁ year, A1, 0.3%	0	3.16	7.23	10.72
X ₅₀ year, A1, 0.3%	0	22.34	51.14	75.78
X ₁ year, A3, 0.3%	0	1.09	3.83	7.13
X ₅₀ year, A3, 0.3%	0	7.69	27.10	50.40

coefficients (after 1 (A1) and 3 (A3) months) for concrete containing different amounts of BFS exposed to an environment containing 0.03 vol.% or 0.3 vol.% CO₂. To detect whether carbonation-initiated corrosion is a risk for the structure within its life span, these values must be compared to the thickness of the concrete cover. In EuroCode 2, the minimum thickness of the concrete covers is specified for XC environments (which are related to carbonation). Since the accelerated carbonation tests were performed at a RH of 60%, which is favourable for carbonation, the values of Table 5 were compared to a concrete cover thickness of 25 mm (applicable in a XC3 environment). The carbonation depths after 50 years for S0 and S50 are acceptable for environments containing 0.03% and 0.3% CO₂, while these of S70 and even S85 are acceptable only if

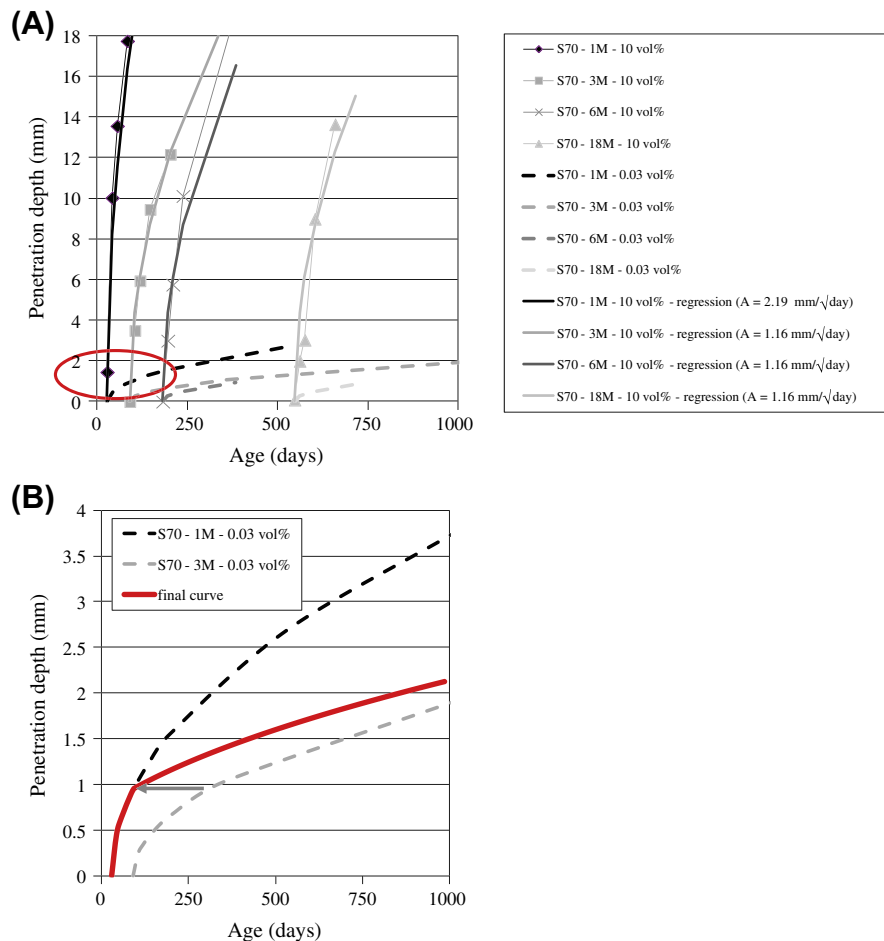


Fig. 6. Determination of the carbonation depth in a 10 vol.% and 0.03 vol.% CO₂ environment in relation with the curing age (1 M, 3 M, 6 M or 18 M). (B) An enlargement of the encircled area of (A).

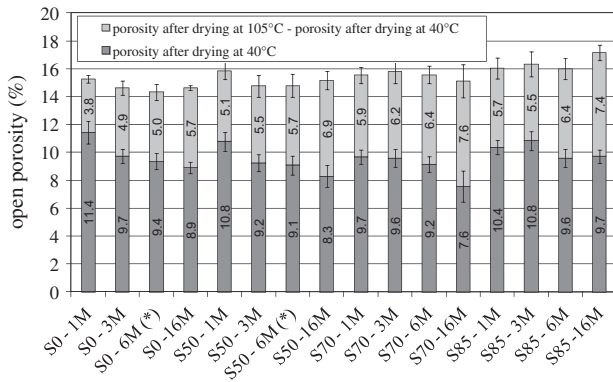


Fig. 7. Open porosity (after drying at 40 °C and 105 °C) of non-carbonated OPC and BFS concrete mixes.

the environment contains small percentages of CO_2 . As the CO_2 content increases up to 0.3%, longer curing periods can limit the carbonation degree of S70 and S85, but not to an extent that the corrosion risk is excluded. In these circumstances, S70 and S85 do not fulfil the requirements. Remark that the carbonation front as determined by the colour change boundary of a phenolphthalein solution does not indicate the maximum front (Section 3.1.4) and a more conservative approach can better take a safety margin into account. Moreover, the actual concrete cover can vary due to construction practices [15]. In order to have a more adequate idea of the actual corrosion risk, a probabilistic service life prediction and risk assessment (which take into account several safety factors) should be performed.

3.1.6. Methodology for including the age effect of concrete with BFS in results from accelerated carbonation tests

From the figures in Table 5, the question arises whether the A1 or A3 carbonation coefficient has to be taken into account to predict the carbonation depth within the concrete's life span. On the one hand, the carbonation depths calculated with A1 are probably too high: the positive effect of the continuing hydration on the carbonation resistance is not taken into account since the carbonation depth which will be obtained in real circumstances after several years is already obtained after a few days in the accelerated carbonation tests. On the other hand, a calculation of $x_{50 \text{ year}}$ with A3 probably underestimates the real value since most of the structures are not cured for 3 months and the worse performance at young ages is neglected.

In Fig. 6, another approach is suggested to determine the carbonation depth in real circumstances (example for S70). First of all, the curves from the accelerated tests are converted with formula (2) to those corresponding with a real environment (CO_2 content of 0.03% assumed in Fig. 6). During the first 2 months (after the concrete is cured for 1 month), it is assumed that the carbonation depth increases with time as indicated by curve 'S70 - 1M-0.03 vol.% CO_2 '. However, at the age of 3 months another curve is available which takes into account the ongoing hydration. Since the concrete was already carbonated over ~ 1 mm (at 91 days), the curve of S70 - 3M-0.03 vol.% CO_2 is shifted to the one of S70 - 1M-0.03 vol.% CO_2 (Fig. 6B). Because the carbonation coefficients at 3, 6 and 18 months are roughly the same, the thick curve (Fig. 6B) can be assumed to be the final one. The values of $x_{50 \text{ years}}$, $A_{\text{final}, 0.03\%}$ obtained in this way (2.47, 8.61 and 16.00 for respectively S50, S70 and S85) are then only slightly higher than those obtained by using A3.

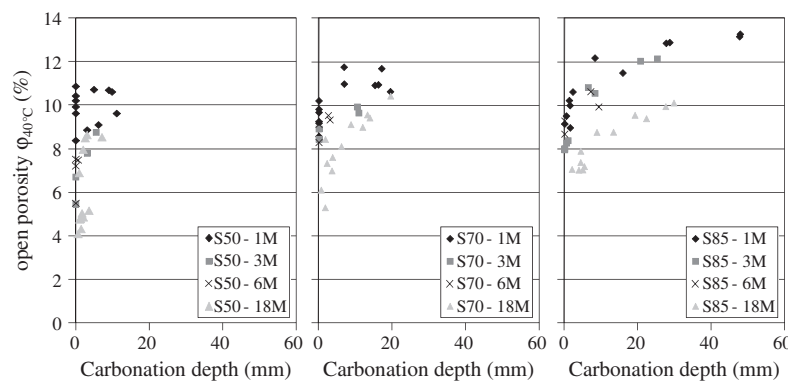


Fig. 8. Open porosity (after drying at 40 °C for 14 days) as a function of the carbonation depth.

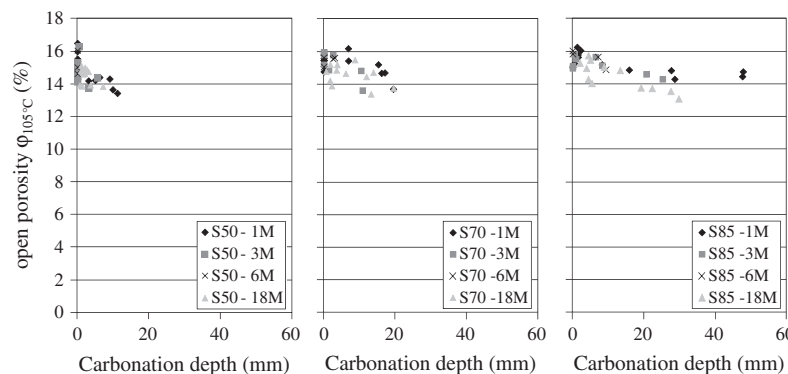


Fig. 9. Open porosity (after drying at 105 °C until constant mass) as a function of the carbonation depth.

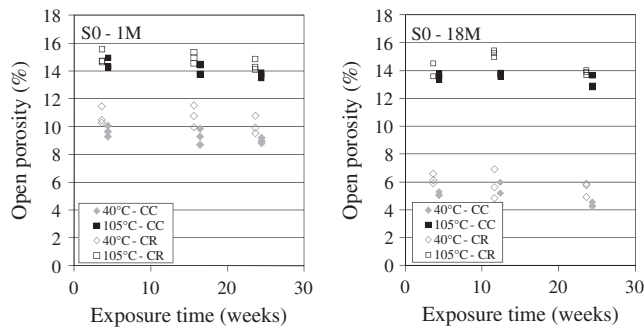


Fig. 10. Effect of the ingress of CO_2 on $\phi_{40^\circ\text{C}}$ and $\phi_{105^\circ\text{C}}$ for OPC concrete. CC (=carbonation cabinet): test specimens exposed to an environment containing 10 vol.% CO_2 at 20°C and 60% RH at an age of 1 (left) or 18 (right) months; CR (=climate room): test specimens which have been stored in a climate room at 20°C and > 95% RH.

Note that the A3 values are obtained from test specimens which were cured for 3 months at 20°C and >95% RH. In real circumstances, curing will not last as long and the actual carbonation depths will be somewhere in between x_{A1} and x_{A3} . Therefore, we propose a test procedure which will allow to calculate realistic carbonation depths: cure the test specimens for e.g. one or a few weeks at 20°C and >95% RH, then store them in a climate room at 20°C and 60% RH and determine the values of A at different ages using an accelerated carbonation test. Subsequently, apply the procedure described above to combine the carbonation curves for various ages into a more realistic curve.

3.2. Influence of carbonation on the pore structure

3.2.1. Pore structure of non-carbonated OPC and BFS concrete

As can be seen in Fig. 7, the mean values of open porosity after drying at 40°C ($\phi_{40^\circ\text{C}}$) and after drying at 105°C ($\phi_{105^\circ\text{C}}$) generally decrease slightly with time while the difference between $\phi_{105^\circ\text{C}}$ and $\phi_{40^\circ\text{C}}$ increases. The ratio of $\phi_{40^\circ\text{C}}$ over $\phi_{105^\circ\text{C}}$ decreases, while the ratio $(\phi_{105^\circ\text{C}} - \phi_{40^\circ\text{C}})$ over $\phi_{105^\circ\text{C}}$ increases with increasing age for each of the mixtures. This indicates that the pore structure refines. Moreover, the values of the ratios $(\phi_{105^\circ\text{C}} - \phi_{40^\circ\text{C}})$ over $\phi_{105^\circ\text{C}}$ are also higher for BFS concrete than for the reference concrete. For BFS concrete, no clear relation could be found between the values of $\phi_{40^\circ\text{C}}$ and $\phi_{105^\circ\text{C}}$ and the slag content.

A statistical analysis (a one-way ANOVA and a Student–Newman–Keuls Post Hoc test was performed since an univariate multi-way ANOVA showed that the interaction between the cement replacement percentage and the age was significant) allows to determine the significant differences as a function of the concrete composition and test age. From this analysis, it could be roughly concluded that, although the total open porosity ($\phi_{105^\circ\text{C}}$) of S0 is significantly lower than that of S50, S70 and S85, $(\phi_{105^\circ\text{C}} - \phi_{40^\circ\text{C}})$ is significantly higher for BFS concrete.

3.2.2. Effect of carbonation

To detect the influence of carbonation on the porosity of OPC and BFS concrete, vacuum saturation tests were performed on concrete test specimens which were stored either in the carbonation cabinet or in the climate room (20°C and >95% RH) after curing. As shown in Figs. 8 and 9, water porosity tests can give interesting information concerning the effect of carbonation and the results

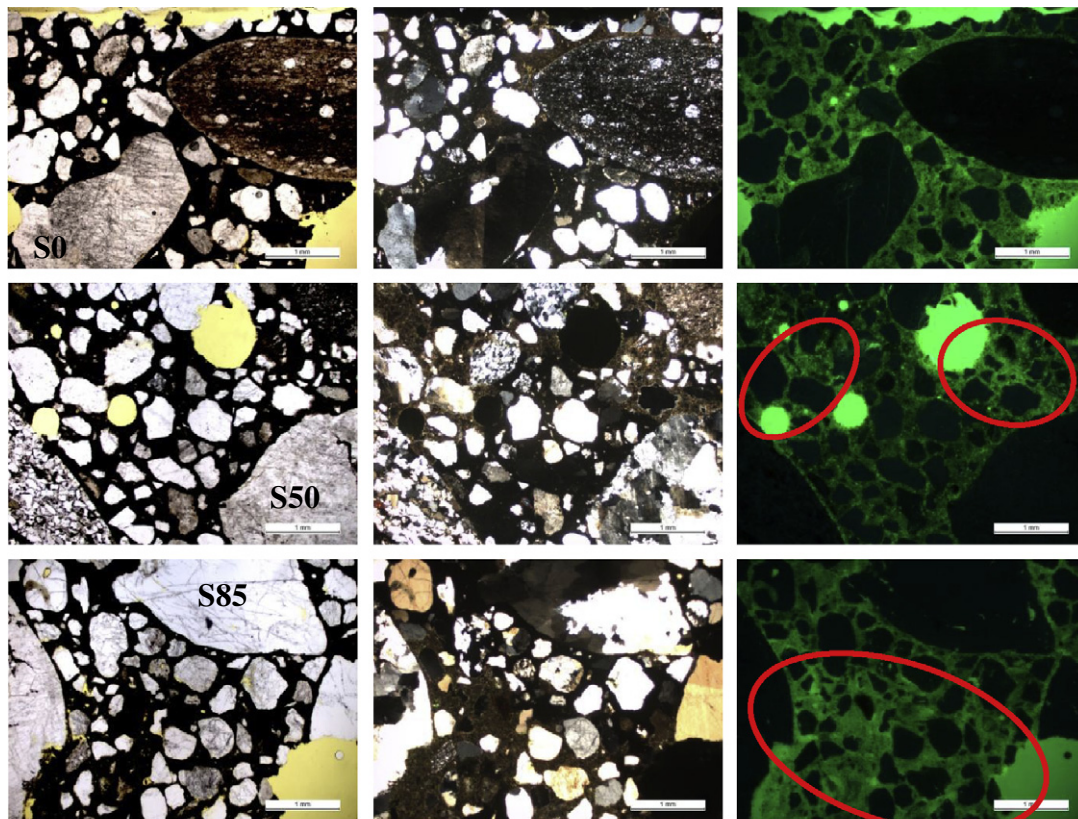


Fig. 11. Microscopic investigation of test specimens exposed to a 10 vol.% CO_2 environment (left: transmitted light, middle: crossed polars (carbonated zone = brown), right: fluorescence microscopy (a higher intensity (encircled) corresponds to a higher capillary porosity)) (—=1 mm). (For interpretation of the references to colour in this figure legend, the reader is referred to the web version of this paper.)

revealed a relation between the open porosity after preparatory drying at 40 °C (for 14 days) or 105 °C (until constant mass) and the carbonation depth for BFS concrete. Moreover, also for the carbonated specimens, a decrease of the open porosity ($\phi_{40^\circ\text{C}}$ and $\phi_{105^\circ\text{C}}$) as a function of curing age can be detected. The effect of an increase in slag content (50 → 85%) is again ambiguous.

For all mixes and curing ages, it is shown that $\phi_{40^\circ\text{C}}$ increases as the carbonation front (determined by the phenolphthalein indicator) progresses. Since higher values of $\phi_{40^\circ\text{C}}$ indicate that more water can evaporate during oven-drying (at 40 °C during 14 days), and thus more water can be absorbed during the subsequent vacuum saturation, the permeability of BFS concrete seems to be increased as carbonation proceeds. Carbonated BFS concrete becomes thus more susceptible to the ingress of aggressive constituents (as e.g. CO₂, chlorides, etc.).

Nevertheless, the total open porosity $\phi_{105^\circ\text{C}}$ slightly decreases (although the measurements show some scatter, this trend can be observed in Fig. 9) as the carbonation depth increases. This means that despite the pore structure is redistributed and becomes coarser, the total open porosity is not negatively affected. According to Borges et al. [10] the reduced overall porosity of BFS pastes after carbonation can be ascribed to pore filling by carbonates.

The increased permeability for BFS concrete indicates that other hydration products than CH are attacked by CO₂ (otherwise a densification of the structure should be obtained since CaCO₃ takes in a higher volume than CH [16]). Because BFS concrete contains merely a low amount of CH (in comparison to OPC concrete) and the C/S ratio of the hydration products is lower than in OPC concrete (due to the lower CaO content and higher SiO₂ content of BFS in comparison to OPC), BFS concrete is especially susceptible to carbonation shrinkage. Silica gel is formed from the condensation of Si–OH groups to Si–O–Si linkages and this reaction is accompanied by shrinkage.

As mentioned above, no carbonation was recorded (by a phenolphthalein indicator) for the reference OPC concrete, even when the specimens were exposed in the carbonation cabinet. However, as can be seen in Fig. 10, exposure to a 10 vol.% CO₂ environment yields values of $\phi_{40^\circ\text{C}}$ and $\phi_{105^\circ\text{C}}$ which are slightly lower than those obtained for reference samples which were further cured at 20 °C and >95% RH. This means that (although no carbonation was detected by a phenolphthalein indicator) the specimens were already partly carbonated and carbonation of OPC concrete is associated with a refinement of the pore structure.

The findings as presented above were confirmed by microscopic investigation of thin sections. Since the specimens were impregnated with fluorescent epoxy and the intensity of fluorescence of the cement paste is a function of the capillary porosity (NT Build 361 (1991)), the difference in porosity between carbonated and non-carbonated zones could be assessed by optical microscopy. In Fig. 11, three examples (S0, S50 and S85) are presented. While the intensity of the fluorescence is about the same in the carbonated and the non-carbonated zones for the reference concrete, BFS concrete shows a higher capillary porosity (and thus a higher fluorescence) in the carbonated zones than in the non-carbonated zones.

4. Conclusion

In this paper, carbonation of BFS concrete and its effect on the pore structure are described.

- The carbonation coefficients increase as the replacement of cement by slag in the concrete increases. The carbonation resistance of BFS concrete is poor and although curing for longer times (up to 3 months) increases the resistance, the

performance remains low, especially for cement replacement levels of 70% and above.

- The carbonation depths as determined by spraying phenolphthalein solution on a freshly sawn surface or by optical microscopy were compared. Since phenolphthalein is a pH indicator, with a colour change at ~pH 9, concrete can be partially carbonated beyond the colour change boundary. This can then be detected by optical microscopy. For the reference mixtures, which showed no carbonation based on phenolphthalein spraying, a very small (0.1–0.7 mm) carbonated zone could be observed by optical microscopy. For the BFS mixes, optical microscopy showed a carbonation front which has (in most of the cases) progressed further into the specimen (up to 3 mm) than the front measured by spraying phenolphthalein solution.
- For BFS concrete, the curing time has a significant influence on the carbonation resistance. A methodology to include the age effect of concrete with SCMs in results of accelerated carbonation tests is proposed. Therefore, accelerated carbonation tests are performed at different curing times. Combination of the decreasing carbonation coefficients as a function of curing time allows to predict the carbonation depth at the end of the service life of the construction more accurately.
- The carbonation depth after a service life of 50 years was estimated based on the carbonation coefficients from the accelerated tests. The results show that, although S50 has a high carbonation coefficient, steel corrosion can be prevented in normal environments. For environments containing merely 0.03% CO₂, S70 and S85 are also satisfactory. When the CO₂ content increases up to 0.3%, longer curing periods can limit the carbonation degree of S70 and S85, but not to an extent that the corrosion risk is excluded. Note that a complete risk analysis should be performed to obtain reliable results.
- Vacuum saturation tests indicate that the open porosity $\phi_{40^\circ\text{C}}$ of BFS concrete increases as carbonation proceeds, while the total open porosity $\phi_{105^\circ\text{C}}$ slightly decreases. This indicates that the pore structure is reorganised and becomes coarser as BFS concrete carbonates, facilitating the ingress of CO₂. For OPC concrete, a slight decrease of $\phi_{40^\circ\text{C}}$ and $\phi_{105^\circ\text{C}}$ was recorded in case of carbonation. The results were confirmed by fluorescence microscopy.
- The vulnerability to carbonation of BFS concrete was attributed to the high gas permeability and the low CH content. Besides CH, other hydration products were also decalcified and because of the low C/S ratio of these hydration products, BFS concrete is especially vulnerable to carbonation shrinkage. As a consequence, the ingress of CO₂ is facilitated and the carbonation process proceeds. In OPC concrete, it is believed that the formation of CaCO₃ causes pore blocking (since CaCO₃ takes a higher volume than CH), which prevents further carbonation.

References

- [1] Robeyst N, Gruyaert E, Grosse CU, De Belie N. Monitoring the setting of concrete containing blast-furnace slag by measuring the ultrasonic P-wave velocity. *Cem Concr Res* 2008;38:1169–76.
- [2] Gruyaert E, Van den Heede P, Maes M, De Belie N. Investigation of the influence of blast-furnace slag on the resistance of concrete against organic acid or sulphate attack by means of accelerated degradation tests. *Cem Concr Res* 2012;42:173–85.
- [3] Gruyaert E, Robeyst N, De Belie N. Study of the hydration of Portland cement blended with blast-furnace slag by calorimetry and thermogravimetry. *J Therm Anal Calorim* 2010;102:941–51.
- [4] Gruyaert E. Effect of blast-furnace slag as cement replacement on hydration, microstructure, strength and durability of concrete. PhD, University of Ghent, Ghent; 2011.
- [5] Baert G, Hoste S, De Schutter G, De Belie N. Reactivity of fly ash in cement paste studied by means of thermogravimetry and isothermal calorimetry. *J Therm Anal Calorim* 2008;94:485–92.

- [6] Baert G. Physico-chemical interactions in Portland cement–(high volume) fly ash binders. PhD, Ghent University, Ghent; 2009.
- [7] Audenaert K. Transport mechanisms in self-compacting concrete related to carbonation and chloride penetration (in Dutch). PhD, Ghent University, Ghent; 2006.
- [8] RILEM CPC 18. Measurement of hardened concrete carbonation depth, RILEM draft recommendation. *Mater Struct* 1984;17:435–40.
- [9] TC 56 – MHM Hydrocarbon Materials. CPC-18 Measurement of hardened concrete carbonation depth. *Mater Struct* 1988;21:453–5.
- [10] Borges PHR, Costa JO, Milestone NB, Lynsdale CJ, Streatfield RE. Carbonation of CH and CSH in composite cement pastes containing high amounts of BFS. *Cem Concr Res* 2010;40:284–92.
- [11] Audenaert K, Boel V, De Schutter G. Carbonation of self-compacting concrete. In: 6th International symposium of utilization of high strength/high performance concrete. Leipzig; 2002. p. 853–862.
- [12] Gruyaert E, Van den Heede P, Maes M, De Belie N. A comparative study of the durability of ordinary Portland cement concrete and concrete containing (high) percentages of blast-furnace slag. In: Bramehuber W, editors. International RILEM conference on material science. Aachen; 2010. p. 241–51.
- [13] Hamada M. Neutralization (carbonation) of concrete and corrosion of reinforcing steel. In: Japan TCAo, editor. 5th International symposium on cement chemistry. Tokyo, Japan; 1968. p. 343–69.
- [14] Thiery M, Villain G, Dangla P, Platret G. Investigation of the carbonation front shape on cementitious materials: effects of the chemical kinetics. *Cem Concr Res* 2007;37:1047–58.
- [15] Fib CEB-FIP. Model code for service life design. In: International federation for structural concrete (FIB). Switzerland; 2006. p. 110.
- [16] Sisomphon K, Copuroglu O, Fraaij ALA. Development of blast-furnace slag mixtures against frost salt attack. *Cem Concr Compos* 2010;32:630–8.